

Coagulation Method for Preparing Single-Walled Carbon Nanotube/Poly(methyl methacrylate) Composites and Their Modulus, Electrical Conductivity, and Thermal Stability

FANGMING DU,¹ JOHN E. FISCHER,² KAREN I. WINEY²

¹Department of Chemical and Biomolecular Engineering, University of Pennsylvania, Philadelphia, Pennsylvania 19104-6315

²Department of Materials Science and Engineering, University of Pennsylvania, Philadelphia, Pennsylvania 19104-6272

Received 14 April 2003; revised 18 July 2003; accepted 21 July 2003

ABSTRACT: A coagulation method providing a better dispersion of single-walled carbon nanotubes (SWNTs) in a polymer matrix was used to produce SWNT/poly(methyl methacrylate) (PMMA) composites. Optical microscopy and scanning electron microscopy showed an improved dispersion of SWNTs in the PMMA matrix, a key factor in composite performance. Aligned and unaligned composites were made with purified SWNTs with different SWNT loadings (0.1–7 wt %). Comprehensive testing showed improved elastic modulus, electrical conductivity, and thermal stability with the addition of SWNTs. The electrical conductivity of a 2 wt % SWNT composite decreased significantly ($>10^5$) when the SWNTs were aligned, and this result was examined in terms of percolation. © 2003 Wiley Periodicals, Inc. *J Polym Sci Part B: Polym Phys* 41: 3333–3338, 2003

Keywords: single-walled carbon nanotube (SWNT); thermoplastic; nanocomposite; electrical conductivity; thermal stability

INTRODUCTION

Carbon nanotubes have shown exceptional stiffness and strength and remarkable thermal and electrical properties, which make them ideal candidates for the development of multifunctional material systems. Previous research has demonstrated the fabrication and characterization of carbon nanotube/polymer composites.^{1–8} For example, Haggemueller et al.⁶ used solvent casting followed by melt mixing to produce single-walled carbon nanotube (SWNT)/poly(methyl methacrylate) (PMMA) composite fibers with enhanced elastic modulus and electrical conductivity.

Barraza et al.⁷ made SWNT/polystyrene composite films with high electrical conductivity with a miniemulsion polymerization method. Kashiwagi et al.⁸ reported that multiwalled carbon nanotube (MWNT)/polypropylene composites made by a shear mixing method showed a significant increase in the decomposition temperature because of the presence of the nanotubes.

However, although remarkable properties of single carbon nanotubes have been reported, nanotube composites have not yet demonstrated their theoretical potential. One of the biggest challenges is obtaining a uniform dispersion of nanotubes in a polymer matrix because carbon nanotubes tend to bundle together even after attempts are made to disperse them.

In this article, a new and versatile fabrication method called *coagulation* is presented; this

Correspondence to: K. I. Winey (E-mail: winey@lrsm.upenn.edu)

Journal of Polymer Science: Part B: Polymer Physics, Vol. 41, 3333–3338 (2003)
© 2003 Wiley Periodicals, Inc.

method achieves a better dispersion of SWNTs in a polymer matrix. SWNTs have been used in this work because they have better properties than MWNTs. The resulting composites exhibit larger elastic modulus, higher electrical conductivity, and increased thermal stability with respect to pure PMMA.

EXPERIMENTAL

PMMA (molecular weight = 100,000 g/mol; Polysciences) was chosen as the matrix polymer because of its good spinning qualities and solubility in dimethylformamide (DMF). SWNTs for the PMMA composites were synthesized by a high-pressure carbon monoxide (HiPco) method (Rice University)⁹ and were purified by the method described by Zhou et al.¹⁰ The metal residue in the SWNTs after purification was less than 8 wt %. The wet purified nanotubes were then dispersed in DMF; this was followed by a filtration step used to get rid of the residual water. The nanotube-PMMA composites are denoted $x\%$ pSWNT/PMMA, where $x\%$ refers to the weight fraction of SWNTs in the composite and pSWNT refers to purified SWNT.

The coagulation method was used to produce the pSWNT/PMMA composites. pSWNTs were added to DMF to give a concentration of 0.25 mg of pSWNT/mL of DMF. A sonication bath (260 W and 45 kHz) was used for 24 h to disperse the pSWNTs in DMF. On the basis of the desired weight fraction of pSWNT in the final composite, an appropriate quantity of PMMA was dissolved in the pSWNT and DMF mixture. The suspension was then dripped into a large amount of distilled water ($V_{\text{DMF}}/V_{\text{water}} = 1:5$) in a blender. PMMA precipitated immediately because of its insolubility in the DMF/water mixture. The precipitating PMMA chains entrapped the pSWNTs and prevented pSWNTs from bundling again. After filtration and drying *in vacuo* at 120 °C for 24 h, the raw pSWNT/PMMA composites were obtained.

For comprehensive testing, three types of composite samples were prepared: fibers, aligned composites, and unaligned composites. The composite fibers were made by melt spinning with a single spinner hole (diameter = 500 μm). The extruded composite fiber was air-cooled and drawn under tension with a windup spool. The diameter of the composite fibers varied from 30 to 50 μm , as determined with a micrometer and an optical microscope. A heat gun was used to weld

the composite fibers together while they were still on the windup spool. These welded fibers were then cut to size and stacked into a channel die. The channel die was then placed onto a hot press (1000 lbs. and 160 °C for ca. 3 min) to produce an aligned composite with dimensions of 2 mm \times 2 mm \times 10 mm. The unaligned composite was made via hot pressing in the same channel die with the raw pSWNT/PMMA composites. The hot press was also used to prepare composite films approximately 30 μm thick, which we observed with an optical microscope to study the dispersion of pSWNT. Scanning electron microscopy (SEM) was used to investigate the fracture surfaces of the composites.

X-ray fiber diagrams were used to characterize the alignment of pSWNT within the polymer matrix. In principle, both wide-angle X-ray scattering and small-angle X-ray scattering (SAXS) should reveal the texture.¹¹ However, because the nanotube loading in our composite sample was relatively low (0.1–7%) and HiPco materials generally have poor crystallinity, the intensity was dominated by the scattering from the polymer matrix in the wide-angle region ($0.3\text{\AA}^{-1} < q < 2.0\text{\AA}^{-1}$). In the small-angle region ($0.01\text{\AA}^{-1} < q < 0.1\text{\AA}^{-1}$), the amorphous polymer matrix had no large-scale features, and so the scattering intensity was mainly from the form factor scattering of nanotubes and nanotube bundles. SAXS unambiguously revealed the texture on which we focused. Measurements were performed in transmission on a Penn multiple-angle X-ray scattering apparatus equipped with a two-dimensional wire detector. From the two-dimensional data sets, we integrated along the radial q direction (e.g., $0.02\text{\AA}^{-1} < q < 0.05\text{\AA}^{-1}$) and plotted the intensity versus the azimuthal angle. These data were then fitted with a simple Lorentzian function, the full width at half-maximum (FWHM) of which quantitatively described the degree of nanotube alignment in the composites.

Mechanical testing for the elastic modulus of the composite fibers was performed in tension on an Instron 4206 with a 0.5 N load cell. The fibers were fixed on a testing tab with a gauge length of 25.4 mm and were tested at room temperature with a deformation rate of 1 mm/min. For both the unaligned and aligned composites, electrical conductivities greater than 10^{-8} S/cm were measured by a four-probe method at room temperature, whereas smaller conductivities were measured by a two-probe method at room temperature. The electrical conductivity of the aligned

sample was measured along the fiber direction, that is, along the nanotube orientation. Thermogravimetric analyses were performed with a TA Instruments SDT 2960 at 5 °C/min from 25 to 800 °C in air with samples (ca. 2.0 mm³) cut from the unaligned composites.

RESULTS AND DISCUSSION

Figure 1(a) is an optical micrograph of a 1% pSWNT/PMMA composite thin film made by the coagulation method. There are no obvious agglomerations of the SWNTs, and this indicates that the nanotubes are uniformly distributed within the polymer matrix on a micrometer scale. On the basis of the SEM image of a 7% pSWNT/PMMA fracture surface shown in Figure 1(b), the diameters of the nanotube bundles are approximately 20 nm, and they are uniformly distributed on a submicrometer scale. In our coagulation method, the polymer chains entrap the surrounding nanotube bundles as the composite precipitates in the DMF/water system because the conformation of the polymer chains changes from a relatively expanded state in DMF to a collapsed state in the DMF/water mixture. Figure 1(c), taken from Haggenueller et al.,⁶ shows an optical micrograph of a 1% pSWNT/PMMA composite thin film made by solvent casting followed by melt mixing. Comparing Figure 1(a,c), we can see that in Figure 1(c) there are numerous agglomerates approximately 10 μm in size. These images indicate that the coagulation method provides a better dispersion of pSWNTs in the polymer matrix. The coagulation method appears to prevent the rebundling of nanotubes after sonication, and the dispersion is comparable to that in the solvent. In contrast, the nanotubes apparently rebundle during solvent evaporation in our previous solvent-casting method.

The nanotube purification process also affects the dispersion of the nanotubes in the composites. At the end of our purification of SWNT, deionized water was used to wash the nanotubes. Because pSWNTs have a better dispersion in DMF than in water, the remaining water had to be eliminated from pSWNTs. After drying pSWNTs *in vacuum* at room temperature, we find that these completely dried nanotubes exhibit poor dispersion in DMF. Consequently, the resulting composite exhibits inhomogeneous pSWNT distribution via optical microscopy (Fig. 2). The numerous black spots in Figure 2 are nanotube agglomerates that

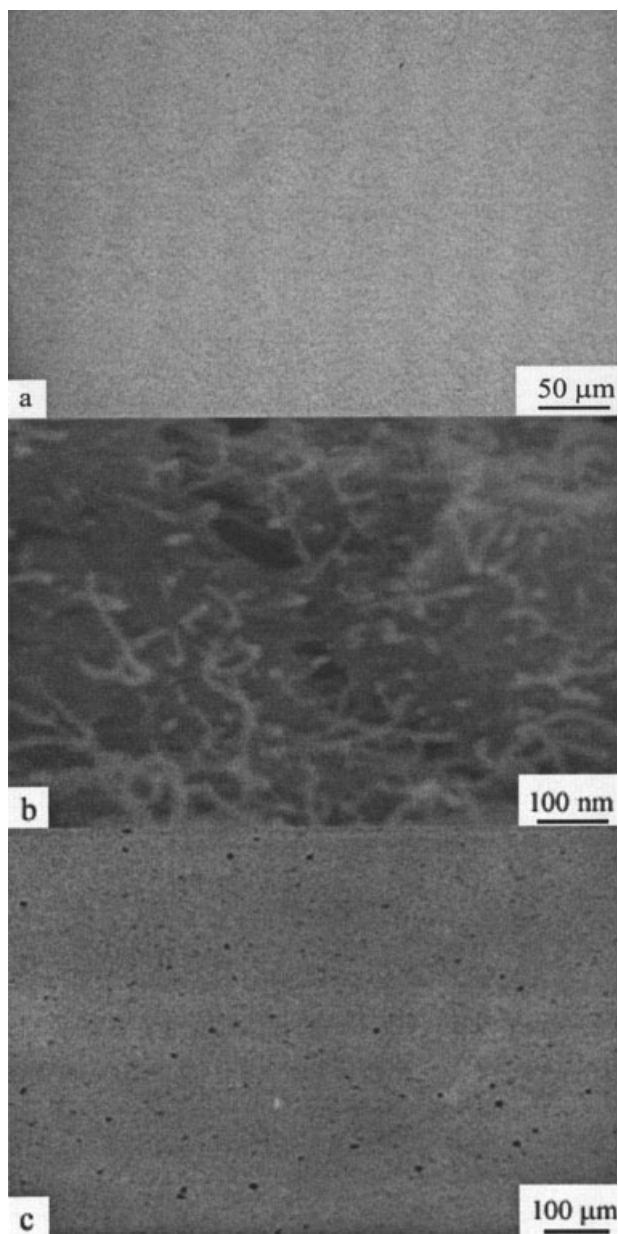


Figure 1. (a) Optical micrograph, showing a uniform SWNT distribution, of a 1% pSWNT/PMMA composite thin film fabricated by the coagulation method; (b) an SEM image, showing a good SWNT distribution, of a 7% pSWNT/PMMA composite fiber fracture surface also prepared by the coagulation method; and (c) an optical micrograph, showing aggregation of pSWNT, of a 1% pSWNT/PMMA composite thin film fabricated by solvent casting from DMF and melt mixing. (From R. Haggenueller et al., *Chem Phys Lett*, 2000, 330, 219, reproduced by permission.)

could not be separated by sonication in DMF after the pSWNT was completely dried. As a result, drying after purification leads to bad dispersion

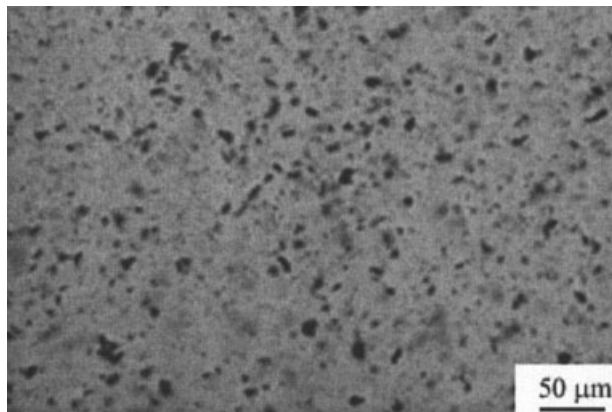


Figure 2. Optical micrograph, indicating considerable pSWNT agglomeration, of a 1% pSWNT/PMMA composite thin film made by the coagulation method with dry pSWNT.

in the final composites. Thus, we exchange the water with DMF in the pSWNT and proceed with the coagulation method, as described in the Experimental section.

The coagulation method can be used not only to produce nanotube–polymer composites but also to produce other nanoparticle–polymer composites. This method can even be applied to a continuous operation in large-scale production. Furthermore, it is applicable to a wide range of thermoplastics, given an appropriate combination of solvents.

SAXS provides a measure of the alignment of pSWNTs in the composites, which makes it possible to study the influence of the alignment of the nanotubes on the properties of the composites. Figure 3 shows fairly good alignment with an

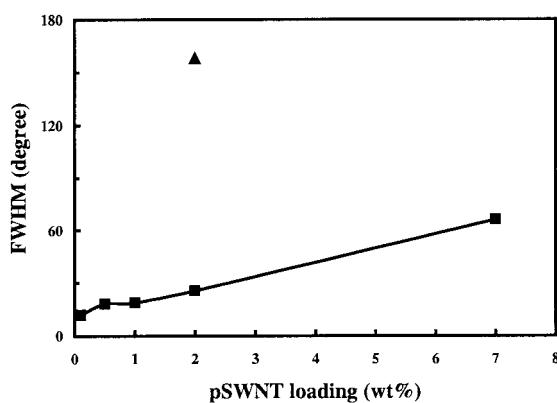


Figure 3. FWHM of the Lorentzian function fitted to the azimuthal distribution of the SAXS intensity from pSWNT/PMMA composites, both (▲) unaligned and (■) aligned, as a function of the pSWNT loading.

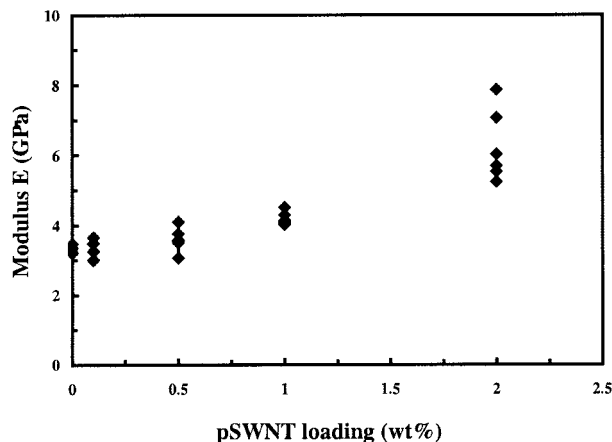


Figure 4. Elastic tensile modulus of pSWNT/PMMA composite fibers as a function of the pSWNT loading.

FWHM of approximately 18° for the 1% pSWNT/PMMA aligned composite. The FWHM increases with increasing pSWNT loading, and this is consistent with the polarized Raman spectroscopy results for the pSWNT/PMMA composite fibers, as reported in Haggemueller et al.¹² As the pSWNT loading increases, the ability to align the small nanotube bundles decreases because of steric constraints imposed by these high aspect ratio objects. Figure 3 also shows that the FWHM of the 2% unaligned composite is approximately 160° , confirming a nearly random orientation of pSWNTs in the polymer matrix.

The elastic modulus increases with the pSWNT loading in the composite fibers, as shown in Figure 4. For example, the average elastic modulus of the 2% composite fiber is approximately 6.3 GPa, which is approximately 90% higher than that of the pure PMMA fibers. Although Haggemueller et al.⁶ previously reported an increase in moduli with the nanotube loading in pSWNT/PMMA composite fibers, our observed increase is more pronounced. For example, similar elastic moduli were measured for 2 and 8% pSWNT/PMMA composite fibers prepared by coagulation and solvent casting with a melt-mixing method, respectively. The improved mechanical properties are probably due to the improved dispersion of the nanotubes within PMMA. The apparently improved dispersion also correlates with the higher viscosity of these composites, which prevents melt-spinning fiber composites with more than 2% pSWNT. Note that Haggemueller et al.⁶ were able to melt-spin fiber composites with up to 8% pSWNT.

With respect to PMMA, the electrical conductivity of the 2% unaligned composite increases by 11 orders of magnitude, up to approximately 10^{-4} S/cm (Fig. 5). The electrical conductivity remains approximately constant for the composites with the higher nanotube loading and exhibits a percolation threshold of approximately 1%. The composition dependence of the electrical conductivity implies that a nanotube network spans the composite at nanotube loadings higher than this threshold. Consequently, adding more nanotubes does not significantly alter the electrical conductivity.

Several other groups have also reported an increase in the electrical conductivity for SWNT/polymer composites. For example, Barraza et al.⁷ reported an increase in the electrical conductivity of an SWNT/polystyrene composite from 10^{-16} S cm^{-1} with a 4% nanotube loading to 10^{-6} S cm^{-1} with a 8.5% nanotube loading, corresponding to a threshold of approximately 6%. Benoit et al.¹³ reported a threshold of 0.33% for the electrical conductivity of an SWNT/PMMA composite film approximately 10 μm thick. Nanotubes confined to a film might be able to form a network at lower nanotube loadings because the nanotubes may not be isotropic. Figure 5 demonstrates the influence of nanotube alignment by comparing the electrical conductivity of the aligned (ca. 10^{-10} S/cm) and unaligned (ca. 10^{-4} S/cm) 2% pSWNT/PMMA composites. This indicates that the alignment of the nanotubes in the composite worsens the electrical conductivity and also shifts the percolation threshold. The reason for the decrease in the electrical conductivity is that there are fewer contacts between the nanotubes when they are

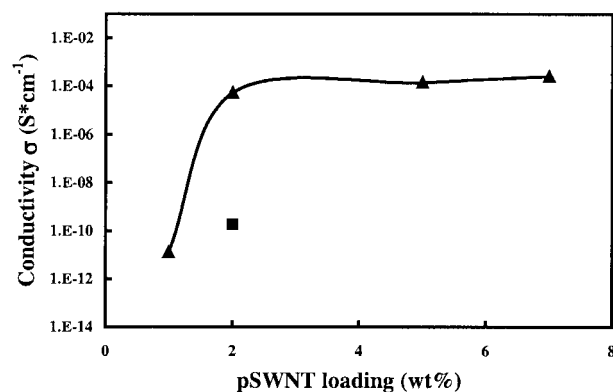


Figure 5. Electrical conductivity of pSWNT/PMMA composites, both (\blacktriangle) unaligned and (\blacksquare) aligned, as a function of the pSWNT loading.

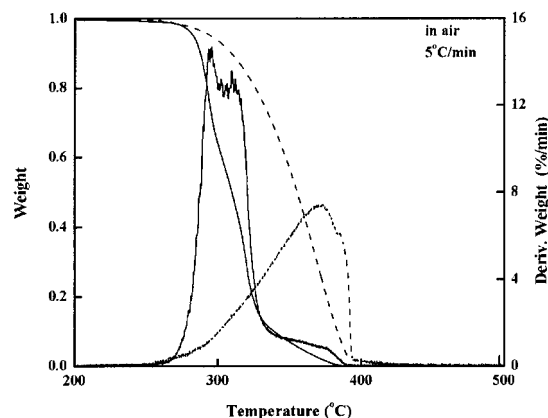


Figure 6. Thermogravimetric analyses of the normalized weight loss and its rate by the initial sample weight at a heating rate of 5 $^{\circ}\text{C}/\text{min}$ in air: (—) pure PMMA and (---) 0.5% pSWNT/PMMA composite.

aligned, and so aligned composites require more nanotubes to reach the percolation threshold. The nanotube orientation, dispersion, and length will also influence the electrical conductivity threshold.

Embedding the nanotubes into the polymer matrix also improves the thermal stability of the polymer, as shown in Figure 6. PMMA and the 0.5% pSWNT/PMMA unaligned composite begin to lose weight at the same temperature, but the temperature at the maximum mass loss rate is 372 $^{\circ}\text{C}$ for the composite, which is approximately 61 $^{\circ}\text{C}$ higher than that for PMMA. Furthermore, the maximum mass loss rate is only approximately 7.8%/min for the 0.5% composite but is 14.5%/min for PMMA. Similar results were found for the other pSWNT/PMMA composites (0.1, 1, and 5%). The improved thermal stability of PMMA through the addition of pSWNT is consistent with recent results showing improved fire retardation.¹⁴

CONCLUSIONS

In summary, a coagulation method was designed and implemented to obtain an improved dispersion of pSWNTs within a PMMA matrix, as shown in optical and SEM micrographs. Extensional flow during melt fiber spinning aligned the pSWNTs according to SAXS. These composites exhibited improvements in mechanical, electrical, and thermal stability properties in comparison with our earlier pSWNT/PMMA composites. The

alignment of the nanotubes in the polymer matrix greatly influenced the electrical conductivity of the composites; the aligned composite was 5 orders of magnitude lower in its electrical conductivity than that of the unaligned composite with the same pSWNT loading. A nanotube network that formed in the composites limited the ability to melt-spin fibers and increased the electrical conductivity and thermal stability.

This research was supported by an Office of Naval Research grant (N00014-00-1-0720) and a Defense University Research Initiative on Nano Technology grant (N00014-01-1-0789). The authors thank R. Haggemueller, W. Zhou, M. Hsu, J. Vavro, and C. Guthy for valuable discussions and assistance with the experiments. The authors are grateful to Rice University for providing HiPco SWNT.

REFERENCES AND NOTES

1. Thostenson, E. T.; Ren, Z.; Chou, T. W. *Compos Sci Technol* 2001, 61, 1899.
2. Thostenson, E. T.; Li, W. Z.; Wang, Z. D.; Ren, Z. F.; Chou, T. W. *J Appl Phys* 2002, 91, 6034.
3. Fisher, F. T.; Bradshaw, R. D.; Brinson, L. C. *Appl Phys Lett* 2002, 80, 4647.
4. Jia, Z.; Wang, Z.; Xu, C.; Liang, J.; Wei, B.; Wu, D.; Zhu, S. *Mater Sci Eng A* 1999, 271, 395.
5. Stéphan, C.; Nguyen, T. P.; de la Chapelle, L.; Lefrant, S.; Journet, C.; Bernier, P. *Synth Met* 2000, 108, 139.
6. Haggemueller, R.; Commans, H. H.; Rinzler, A. G.; Fischer, J. E.; Winey, K. I. *Chem Phys Lett* 2000, 330, 219.
7. Barraza, H. J.; Pompeo, F.; Orear, E. A.; Resasco, D. E. *Nano Lett* 2002, 2, 797.
8. Kashiwagi, T.; Grulke, E.; Hilding, J.; Harris, R.; Awad, W.; Douglas, J. *Macromol Rapid Commun* 2002, 23, 761.
9. Nikolaev, P.; Bronikowski, M. J.; Bradley, R. K.; Rohmund, F. R.; Colbert, D. T.; Smith, K. A.; Smalley, R. E. *Chem Phys Lett* 1999, 313, 91.
10. Zhou, W.; Ooi, Y. H.; Russo, R.; Papanek, P.; Luzzi, D. E.; Fischer, J. E.; Bronikowski, M. J.; Willis, P. A.; Smalley, R. E. *Chem Phys Lett* 2001, 350, 6.
11. Zhou, W.; Winey, K. I.; Fischer, J. E. *Mater Res Soc Symp Proc* 2003, 740, I12.21.1.
12. Haggemueller, R.; Zhou, W.; Fischer, J. E.; Winey, K. I. *J Nanosci Nanotech* 2003, 3, 1.
13. Benoit, J. M.; Corraze, B.; Lefrant, S.; Blau, W.; Bernier, P.; Chauvet, O. *Synth Met* 2001, 121, 215.
14. Kashiwagi, T.; Du, F.; Winey, K. I.; Harris, R. H.; Shields, J. R.; Douglas, J. F. *Macromol Rapid Commun*, submitted for publication, 2003.